

S100A4 down-regulates filopodia formation through increased dynamic instability

Connie Goh Then Sin¹, Nils Hersch³, Philip S. Rudland², Roger Barraclough², Bernd Hoffmann³ and Stephane R. Gross^{1§},

¹School of Life and Health Sciences, Aston University, Aston Triangle, Birmingham B4 7ET, UK.

²From the Institute of Integrative Biology, University of Liverpool, Biosciences Building, Crown Street, Liverpool, L69 7ZB, UK.

³ Institute of Complex Systems, ICS7: Biomechanics; Forschungszentrum Jülich GmbH, Jülich, Germany

§ To whom correspondence should be addressed.

Email: S.R.Gross@aston.ac.uk

Tel: +44 121 2367;

Fax: +44 121 204 4187;

The authors have no competing financial or conflict of interests. This work was partly supported by a Biomedical Science grant from Aston University

Abstract

Cell migration requires the initial formation of cell protrusions, lamellipodia and/or filopodia, the attachment of the leading lamella to extracellular cues and the formation and efficient recycling of focal contacts at the leading edge. The small calcium binding EF-hand protein S100A4 has been shown to promote cell motility but the direct molecular mechanisms responsible remain to be elucidated. In this work, we provide new evidences indicating that elevated levels of S100A4 affect the stability of filopodia and prevent the maturation of focal complexes. Increasing the levels of S100A4 in a rat mammary benign tumour derived cell line results in acquired cellular migration on the wound healing scratch assay. At the cellular levels, we found that high levels of S100A4 induce the formation of many nascent filopodia, but that only a very small and limited number of those can stably adhere and mature, as opposed to control cells which generate fewer protrusions but are able to maintain these into more mature projections. This observation was paralleled by the fact that S100A4 overexpressing cells were unable to establish stable focal adhesions. Using different truncated forms of the S100A4 proteins that are unable to bind to myosin IIA, our data suggests that this newly identified functions of S100A4 is myosin dependent, providing new understanding on the regulatory functions of S100A4 on cellular migration.

Introduction

The formation of secondary tumour at distant metastatic sites from the original site of growth, is a multi step progression which leads to poor prognosis for cancer patients. To acquire invasive properties, tumour cells undergo major changes in shape and motility. Significant changes in localised actin structures at the leading edges of tumour cells with polymerisation and depolymerisation under dynamic control ¹ allow them to protrude thin sheet-like lamellipodia ² or needle-like membrane extensions called filopodia. Filopodia are highly dynamic structures that extend and retract over very short time frames which act as sensory organelles for the extracellular matrix or other cells. Their protrusion is powered by actin polymerisation at their tips ³ whilst their overall structure is the result of tightly packed bundles of actin fibres cross linked by fascin ⁴. Such finger-like extensions play essential regulatory roles in cell spreading and adhesion during migration ⁵⁻⁶ through the formation of nascent focal complexes (FX) ⁶⁻⁸. Proper organisation of these FX, and more importantly, tight adhesion to external cues through interactions of transmembrane receptors such as integrins or cadherin ⁵, result in the maturation of the complex into canonical focal adhesions (FA). Maturation of FA is accompanied by a large increase in their size, during a timely regulated process where markers like paxillin and vinculin, among numerous others ⁹, interact at these focal contacts with each other and with actin stress fibres and integrins to provide a link to the extracellular matrix. Importantly, kinetic analyses have recently demonstrated the involvement of myosin II in the timely maturation of FX and FA ^{7, 10-11}. The biological mechanisms deciphering how myosin II functions in FA maturation remain to be fully unravelled, but could be through either the generation of tension, which directly affects the conformation of proteins in the adhesion complex ¹², or its cross-linking activity ^{11, 13}. Consequently, factors that can regulate both myosin II's cross-linking activities and contraction are good candidates to govern FA formation ¹³⁻¹⁵.

One factor known to influence myosin activity is the small calcium binding EF-hand protein S100A4. S100A4 can bind to the heavy chain of myosin IIA both *in vitro* and *in vivo* ¹⁶⁻¹⁹ where it promotes the disassembly of pre-existing filaments ²⁰ or their actual assembly ²¹. It is thought that such recruitment to the actin/myosin fibres may be directly linked to S100A4's ability to promote cell motility ²²⁻²³ and metastasis ²⁴⁻²⁵. Consistently with this idea, elevated levels of S100A4 in the primary tumour have been correlated to its progression to a metastatic stage and to a poor prognosis for patient survival in breast cancer ²⁶⁻²⁷. S100A4 also induces a metastatic phenotype when transfected into benign rat mammary tumour cells

in a transgene model of breast cancer²⁸⁻²⁹. Both, the C-terminal region of S100A4 and its EF-hand motifs are required for interaction of S100A4 with myosin IIA and abrogation of its Ca²⁺ binding properties or truncation of its C-terminus lead to reduced metastasis promotion^{24-25, 30}.

Whilst a clear link between overexpression of S100A4, cellular motility and metastasis has been established, the biological consequences of elevated S100A4 levels remained elusive at the molecular side and we still lack much of the information regarding the changes taking place at the cellular level to promote migration. In this work, we show that elevated levels of S100A4 affect the stability of filopodia, preventing the maturation of FX/FA. This effect results in immediate retraction of most filopodia and a reduced rate of formation newly formed FX and a low number of matured FAs. Using different truncated forms of the S100A4 proteins which are unable to dimerise and bind to myosin IIA, our data suggest that this newly identified function of S100A4 is dependent on myosin, thus provide new understanding on the molecular mechanisms underpinning the ability of S100A4 to enhance cellular migration.

Material and Methods

Cell culture and lines

The rat mammary (Rama 37) non-metastatic benign tumour derived cell line³¹ expresses barely detectable levels of S100A4 mRNA and protein. The four cell lines used during this work were: a) the control cells transfected with the empty pBKCMV vector, b) the cell line transfected with the full length S100A4 open reading frame inserted in the pBKCMV expression plasmid (S100A4WT), c) and d) cell lines S100A4Δ2 and S100A4Δ6 which were obtained by transfection of the expression vectors for S100A4 protein with C-terminal truncations lacking amino acids 100-101 or 96-101 respectively. Both truncations have been shown to affect the ability of S100A4 to bind and interact with myosin IIA heavy chain using Biosensor analysis²⁴⁻²⁵

The cells were routinely cultured in a humidified atmosphere at 37°C, 5% (v/v) CO₂, 95% (v/v) air in Dulbecco minimal Eagle's medium (DMEM) supplemented with 2 mM L-glutamine (50 U per ml) penicillin/streptomycin (50 mg per ml), 10% (v/v) fetal bovine serum (heat inactivated), 5ng/ml insulin and hydrocortisone and 0.8 mg/ml geneticin (G418).

Scratch assay and cell migration measurement

Cell migration of the various cell clones was assessed using scratch assays. 10⁵ cells were seeded into each well of 12 well tissue culture plates and left to grow for 48 hrs when they reached 90% confluency. Confluent monolayers were scored with a sterile pipette tip to leave a scratch of approximately 0.4-0.5 mm in width. Culture media was removed and replaced with fresh media. Wound closure was monitored by collecting digitalized images at various time intervals after the scratch. Digitised images were captured in phase contrast with inverted epifluorescence microscope (DM14000B, Leica) using a N-Plan 10x /0.25 PH1 objective. Digitised images were also obtained using the Cell IQ automated image capture system, (Chip-Man Technologies, Tampere, Finland) in which pre-selected fields were imaged using phase contrast microscopy on a continuous loop until wound closure was complete. The Cell-IQ Analyser Software, using Machine Vision Technology, was able to detect and measure remaining areas deprived of cells/migrating sheets. Data from this equipment has been presented as the velocity of wound closure, i.e. the time that was required for full closure to be completed.

Immunofluorescence staining of cultured cells.

Rama 37 cells expressing either wild type S100A4, S100A4 Δ 2, S100A4 Δ 6 or cells transfected with empty pBKCMV vector were plated at a concentration of 1.5×10^4 cells/ well onto fibronectin-coated ($2.5 \mu\text{g}/\text{cm}^2$) glass coverslips in 24-well plates. Cells were grown for 48 hrs prior to being washed once in cytoskeleton buffer (CB: 150 mM NaCl, 5 mM MgCl₂, 5 mM EGTA, 5 mM glucose, 10 mM 2-(N-morpholino) ethanesulfonic acid, pH 6.1) and being fixed with 3.7% (w/v) paraformaldehyde in CB at 37°C for 20 min. Cells were then further washed in CB before being permeabilised with 5% (v/v) Triton X-100 in CB for 2 min and blocked with blocking solution (5% (v/v) goat serum in CB) for 60 min at room temperature. Samples were incubated with primary antibodies vinculin (Sigma, St Louis, USA), paxillin (Invitrogen, Paisley, UK) or fascin (Chemicon, Millipore) (dilution between 1/60, 1/100 and 1/500, respectively) in blocking solution (1% (v/v) goat serum in CB) for 45 min at 37° C. After washing three times with the blocking solution, cells were incubated with the appropriate secondary antibodies, anti-rabbit and anti-mouse antibodies labelled with FITC (Dako, Ely, UK) in blocking solution for 45 min at 37°C with a dilution of 1:100. For actin staining, rhodamine phalloidin (Invitrogen, Paisley, UK) was also added, with the secondary antibodies at a concentration of 0.6 μM . After 3 washings with blocking solution, coverslips were rinsed once with water and mounted in Vectashield mounting medium (Vector, Peterborough, UK) before viewing using a confocal microscope (TCS SP5 II Confocal, Leica) at using HCX PL APO 63x/1.4-0.6 oilCS objective at 20% argon laser intensity.

Live cell analysis.

For live cell analysis, the different cell lines were seeded with density of 5×10^5 cells in a 50mm Petri dish and grown for 24 hours prior to pGZ21 GFP-vinculin expressing plasmid (a kind gift from Benjamin Geiger, Weizmann Institute of Science, Rehovot, Israel) transfection with jetPeiTM. The transfectants were trypsinised and reseeded at a density of 5×10^3 cells into a customised 170 μm -thickness glass bottom Petri dish, pre-coated with $2.5 \mu\text{g}/\text{cm}^2$ of fibronectin (BD Biosciences, Palo Alto, CA) for 30 min at 37°C. The analyses were carried out 24 hours post seeding with a confocal microscope (LSM710, Zeiss) using EC Plan-Neofluar 40x/1.30 Oil Ph3 objective (Zeiss) at 37°C and 5% CO₂. The duration for

single cell analysis was set to 20 min per cell with 10s intervals. Phase contrast and GFP imaging was taken with argon ion laser line with a wavelength of 488nm and 2.4 - 2.8% of laser intensity. All the parameters were kept constant throughout the analyses. Images obtained were optimised (background subtraction and contrast adjustment) with ImageJ for better visualisation.

Analysis of actin organisation

Cells stained with phalloidin were observed using confocal microscopy and large field of cells from each lines were photographed. The average gray value of all cells in an image was determined using segmentation after withdrawing the background threshold. Quantitative analysis of the actin organization was then obtained after collection of all these cell-pixels intensity, resulting in the average gray values.

Statistical analysis

Data presented in this study are listed as mean \pm standard error (s.e.). These data were tested for normal distribution by Kolmogorov–Smirnov test using Analyse-it software. As all data were shown to be normally distributed the student t- test was used to determine significant differences between samples.

Results

Overexpression of S100A4 increases wound healing migration and overall cell motility

The effects of S100A4 overexpression on promoting cell invasion are well documented²³⁻²⁵. We sought to determine whether increased levels of S100A4 proteins in cells could also affect their ability to promote wound closure using the established scratch assay (**Fig.1**). Rama 37 cells stably expressing full length S100A4 or their control counterparts were seeded in 12 well plates, scratched and monitored by time lapse microscopy. Expression of wild type S100A4 led to dramatic changes in cell migration and wound healing repair, with differences in gap closure observed as soon as 2 hrs post scratching (data not shown). Eight hours following injury, the scratch was nearly completely filled in Rama 37 cells expressing high levels of S100A4, whereas control cells had only migrated about 50% across the wound (**Fig. 1A**). Real time dynamics of migration and wound repair were also measured using the CellIQ system and demonstrated that the Rama 37 cells expressing full length S100A4 were much more efficient in closing the wound, requiring nearly half the time than the control counterparts (**Fig. 1B**). To establish whether such properties of S100A4 were linked to its ability to interact with myosin IIA, we tested if expression of nested truncated forms of S100A4 also affected wound closure. Deletion of the last 2 or 6 C-terminal amino acids, referred to as S100A4 $\Delta 2$ and $\Delta 6$ transfected cell lines respectively, have been shown to contain similar levels to wild type S100A4 in the Rama 37 transfected cell system. These truncated forms of S100A4 dramatically reduce the ability of S100A4 to bind to myosin IIA *in vitro*²⁴. Expression of either truncated versions of S100A4 did not accelerate the wound healing process and led to migration/gap closure dynamics similar to that for control cells (**Fig. 1**), demonstrating that the C-terminal portion of S100A4 that is required for myosin IIA binding is equally essential for its ability to promote wound repair.

High level of S100A4 leads to a reduction in focal adhesion formation

Having determined that overexpression of S100A4 leads to an increase in wound repair and cellular motility, we were interested to comprehend what happens at both the cellular and molecular levels to promote such changes. Cellular migration is driven by the

ability of cells to interact with the extracellular matrix, through the formation of focal adhesion (FA) where transmembrane proteins of the integrin type interact with the actin cytoskeleton via adapter proteins like paxillin and vinculin that aggregate early on ⁹. We therefore sought to determine whether high level of S100A4 proteins would lead to changes in the localisation of such foci in the Rama 37 cells. In immunocytochemical experiments clear localisation of paxillin in clusters at the periphery of the cells was observed in the control cells (**Fig. 2A-2A'**). Expression of high level of the full length S100A4 resulted in the total loss of foci formation around the cells (**Fig. 2B-2B'**). Overall actin organisation was also dramatically affected by the expression of S100A4.

Analysis of the average gray value of all cells in an image was determined using segmentation after withdrawing the background threshold. Data from this analysis indicates that cells overexpressing S100A4 have a greater signal ratio (132.5 ± 16.2) compared to all other counterparts ($p < 0.001$), with the control rama37 cells having the lowest (100.5 ± 14.1). Expression of the truncated forms of S100A4 were found to lower the effects on actin organization, revealed by the analysis presenting values at (110.2 ± 13.2) for S100A4 Δ 2 and (117.4 ± 4.6) for S100A4 Δ 6. This data therefore shows that cells overexpressing S100A4 present a more diffuse cytoplasmic levels of actin than the control cells and suggest high remodelling of its organisation, whilst the level of reorganisation was much less obvious when cells were transfected with the truncated forms of the protein.

Number of actin projections were significantly reduced in the cells containing high levels of S100A4. The expression of either S100A4 Δ 2 or S100A4 Δ 6 in Rama 37 cells led to a total reversion of the S100A4 phenotype (**Fig. 2C** and **Fig. 2D** respectively), with a clear recovery of paxillin containing FA and actin organisation similar to that of the control cells. Analysis of another marker for FA formation, vinculin, generated comparable results (data not shown). Taken together, these data demonstrate that expression of S100A4 induces critical changes in both FA formation and actin organisation, including a significant reduction in actin projection and a change in cellular morphology from a filopodia to lamellipodia dependent process. The ability of S100A4 to induce such changes is coincidental with its ability to interact with myosin IIA *in vitro* ²⁴.

S100A4 reduces filopodia formation

The fact that induction of S100A4 expression resulted in significant reduction in actin projections away from the cell stroma prompted us to determine the exact nature of these extensions. Because protrusion of filopodia is powered by actin polymerisation at their tips³ and their overall structure is the result of tightly packed bundles of actin fibres cross-linked by fascin⁴, we analysed the localisation of the fascin protein in the filamentous structures. Immunofluorescent staining for fascin in the 4 different cell lines (**Fig. 3**) and quantitative analysis of the number of those stably attached projections (**Table 1**) were carried out. An average number of 41.2 ± 8.6 protrusions from the cell cortex could be seen in the control cells. Staining for fascin was seen throughout the length of the extension with an accumulation at the tip (**Fig. 3**). Expression of the full length S100A4 led to a dramatic reduction to 3.5 ± 1.5 per cell, with a very small amount of fascin present at the cell periphery. The overall structure of these wild type S100A4 containing cells highlighted the presence of a large leading edge and polarised morphology (**Fig. 3B-B'**). By contrast, Rama 37 cells expressing the truncated forms of S100A4 Δ 2 and S100A4 Δ 6 did not show such a striking change in morphology. Fascin containing filopodia were present throughout the cells with protein localisation similar to that of the control cells (**Fig. 3C-C'** and **Fig. 3D-D**). Quantitative analysis of filopodia in the S100A4 Δ 2 expressing cells resulted in no significant changes in the number of adhered filopodia (31.6 ± 11.3) compared to the control cells, whilst there was a significant decrease in the number in the S100A4 Δ 6 expressing cells (19.7 ± 8.7). All together, these data demonstrate that S100A4 down regulates the number of filopodia and that this ability may be dependent on its myosin IIA binding properties.

Elevation of wild type S100A4 protein expression causes overall reduction in focal adhesion dynamics

Our initial observations using immunofluorescence staining (**Fig.2**) indicated that the number of FA is greatly reduced when the wild type S100A4 protein is overexpressed. We were interested to determine whether such reduction in their formation was due to changes in their dynamicity. To validate this, all cell lines were transfected with GFP-vinculin expressing plasmid and analysed over time by confocal microscopy. A representative image of the control Rama 37 cell is shown in **Fig. 4**. From the collected images, focal contacts which were newly formed within 20 minutes (black arrows) were distinguished from those

that were already present and both sets of information were recorded and analysed (**Table 2**). The quantification analysis shows that Rama 37 control cells, S100A4 Δ 2 and S100A4 Δ 6 expressing cells displayed similarities in overall number of FA present (89.4 ± 13.4 , 93.6 ± 6.3 and 83.6 ± 12.1 respectively). Overexpression of full length S100A4, on the other hand, led to a significant reduction in the number of GFP-vinculin incorporated into FA (50.2 ± 11.5). These results confirmed our data from immunostaining analyses given above.

To assess more specifically the rates of FA assembly, the number of FA formed over 20 minutes was quantified (**Table 2**). The number of FA formed during this time course, in wild type S100A4 protein expressing cells (11.4 ± 3.5), was significantly lower than in cell lines expressing either the S100A4 Δ 2 or S100A4 Δ 6 proteins (28.2 ± 6.9 and 23.6 ± 6.6 respectively). Surprisingly, Rama 37 control cells did not show significant difference in FA formation (14.4 ± 2.1) when compared to wild type S100A4 expressing cells ($P=0.0704$) although the mean value was slightly higher in the former cell line. Except for the Rama 37 control cells, the formation of focal contacts for the other cell lines correlates with the total number of FA present during the 20 minutes time period. However, one needs to keep in mind that for this representative experiment the number of analyzed cells is rather low making it difficult to draw strong conclusions at this point.

Quantification of filopodia on live cells was carried out by randomly halting images at one time point and by monitoring dynamics changes in filopodia and retraction fibres over subsequent times (**Fig.5**). This analysis indicated that wild type S100A4 expressing cells formed a significantly higher number of filopodia compared to S100A4 Δ 6 protein expressing cells and Rama 37 control cells (**Table 2**) in the course of our time course. This suggests that whilst overall number of stabilised filopodia are reduced in the S100A4 overexpressing cells, this is not due to a reduction in their formation, but more possibly due to their fragility and high dynamics. Although the filopodia quantified in S100A4 Δ 2 shows no significant difference, the mean value is still lower than those of wild type S100A4 protein expressing cells (**Table 2**). Since recent work in keratinocytes indicated that FA formation depend on stably adhered filopodia ⁶, we followed stably adhered filopodia containing GFP-vinculin by fluorescence and phase contrast over time (**Fig. 4**, black arrow and **Fig. 5**). These data clearly show that FA are formed along filopodial actin bundles upon contact with the lamellipodium. Furthermore filopodia dependent formation of FAs was detected in all 4 cell lines (see supplementary movies S1-S4 for all cell lines).

Discussion

The S100A4 protein has become a prominent player during cancer progression and the metastasis stage since it is overexpressed at high concentration in a vast repertoire of malignancies ranging from melanoma to non-small cell lung carcinoma and cancers of the breast and stomach ³²⁻³⁵. Whereas S100A4 has not been directly implicated with the tumorigenesis process as its overexpression does not result in uncontrolled cellular growth ³⁶, it is thought that S100A4 is a key player regulating the migration or invasion steps required in the metastatic cascade. Thus high expression of S100A4 increases the migratory properties of transformed fibroblasts and non-metastatic adenocarcinoma cell line ^{23, 37 22}. Conversely, ablation of S100A4 expression in tumour cells correlates with decreased cellular motility ³⁸⁻³⁹. There is little doubt that S100A4 can promote cell migration in both tumour and normal cells, however, the underlying biological mechanism for such changes is still poorly understood. To shed more lights on some of the mechanisms that could explain the gain in migratory properties, we have utilised a non-metastatic rat tumour-derived cell lines transfected with different forms of the S100A4 proteins. We show that forcing high levels of expression of the full length protein results in a significant reduction in the formation of stable and mature focal adhesion (FA) and leads to a dramatic reduction in stable filopodia formation whilst similar cell lines expressing truncated versions of the S100A4 protein that have lost their ability to interact with myosin IIA are unable to induce such alterations.

As cells migrate, they organise their leading edge in 3 chronological steps; these involve the initial formation of cell protrusions (lamellipodia and/or filopodia), attachment of the leading lamella to extracellular cues and formation of focal contacts at the leading edge that mature through the production of tensile forces. Our initial observations have demonstrated the formation of abundant actin containing protrusions at the cell's leading edge (**Fig. 2B, Fig 3B**) in the full length S100A4 overexpressing cells compared to the control counterparts. When two truncated forms of S100A4 which are unable to bind to myosin IIA (mutants S100A4 Δ 2 and S100A4 Δ 6) are overexpressed, they do not induce such changes, suggesting that this induction is probably dependent on myosin IIA. Such findings are consistent with those of Bresnick's works which have shown that S100A4 can induce forward protrusions during chemotaxis ²³ and that enrichment of the myosin IIA-S100A4 complex occurs at the leading edge of polarised cells ⁴⁰. When high levels of wild type S100A4 are induced, significant reorganisation of actin structures also occurs, mainly the loss

of the actin stress fibres and actin arcs. Actin arcs are thought to be formed from actin filaments and bundles that are oriented in the direction of the cell's edge and perpendicular to retrograde F-actin in the lamellipodium⁴¹. These arcs are clearly visible in the control cells, appearing as ring shaped structures but overexpression of the full length S100A4 protein resulted in their abolition (**Fig. 2-3**). Interestingly, the lamella and stress fibres were again clearly visible in cells containing high levels of the truncated forms of S100A4 (mutants S100A4 Δ 2 and S100A4 Δ 6) indicating that S100A4 may regulate their formation through its interaction with myosin IIA. This finding is in agreement with previous work which has shown that myosin IIA has been implicated in regulating the reorganization of actin network in the lamellipodia of spreading cells⁴¹⁻⁴³. Our data suggest that S100A4 may be one of the cellular regulator of such process.

Our data also shows that formation of cellular protrusion is modified upon expression of wild type S100A4 when analysed in fixed cells. Control cells demonstrated a large number of filopodia formation whilst high levels of S100A4 resulted in significant reduction (**Fig, 3 and table 1**). However, fixed cells only allow the characterisation of stably adhered filopodia while unstable ones are lost due to the analysis procedure. By contrast, live cell imaging quantification of filopodia numbers indicated, that in fact, the number of newly formed filopodia in all cells was not greatly affected. In fact, filopodia formation was even accelerated in the presence of high levels of S100A4 (**Table 2**). These data therefore suggest that S100A4 inhibits in some way the adhesion of stably adhered filopodia, although their actual initial formation rate is higher. During formation of filopodia, myosin-X acts as a catalyst by bringing filaments together to facilitate bundling at the actin-membrane interface⁴⁴. S100A4 has so far been shown to interact directly with myosin IIA and, with much less efficiency to IIB but not at all with myosin V^{17, 20}. It is unclear, at this time, whether S100A4 can influence myosin X activity but it is tempting to speculate that such interactions, if true, could induce significant changes in stabilisation and promotion of filopodia.

Previous experiments by Schäfer et al.^{6, 45} using migrating keratinocytes have shown that there is a clear dependence of stable FAs on stably adhered filopodia. Since we could also observe a filopodia dependent formation of FAs and a reduced number of FAs upon expression of S100A4 one is tempted to argue that a similar dependence between filopodia and FAs also exists in our cell types. However, at the current state we cannot finally answer this hypothesis. This is mainly because of the different migration type of our cells compared to the stably polarized migrating keratinocytes used in previous work. Cancer cells as used here permanently form lamellipodial extensions in all directions but barely move the centre

of the cell over time. Therefore, filopodia permanently switch into retraction fibres making it very difficult to distinguish whether FAs are formed right behind filopodia or just enlarge because of a new outgrowth over former retraction fibres. Here, time lapse analyses over very long time frames might solve this question which is out of the scope of this work.

Our analysis therefore demonstrates that high levels of S100A4 induce the formation of many nascent filopodia, but that only a very small and limited number of these can stably adhere. We suggest that this phenomenon is the result of inhibited myosin function leading to filopodia and filopodial complexes that cannot be stabilised. Such possibility is supported by recent findings demonstrating the importance of myosin II in the timely maturation of focal complexes (FX) and FA ^{7, 10-11}. Such lack of maturation would, therefore, lead to filopodial retraction and a low number of FAs resulting in the observed effects on morphology and migration. The reasons for S100A4 to induce such effects through myosin IIA remain to be explicitly demonstrated. It is thought that S100A4 can function as a myosin-IIA inhibitor *in vivo*, since it has been reported to inhibit the actin-activated ATPase of myosin-IIA ¹⁷. Inhibiting the molecular motor properties of myosin IIA would lead to a loss of tension on actin stress fibres, resulting in significant changes in the conformation of proteins in the adhesion complex ¹². Alternatively S100A4 has been shown to impair myosin polymerisation and its organisation into highly defined filaments ¹⁷. The aggregation of myosin IIA into fibres is thought to induce cross-linking activities on adjacent actin filaments, a process that is also required for FX maturation ^{11, 13}. Consequently, high levels of S100A4 could similarly affect FX formation through the disruption of myosin IIA fibres.

Although our data argues that S100A4 may regulate actin arcs arrangements, FX and FA formation as well as filopodia extension through its potential interaction with myosin, given that none of the truncated forms of S100A4 which have impaired myosin binding could reciprocate, there could be other potential candidates that we should factor in for such regulation. Other prospective targets for S100A4 are the cytoskeletal proteins, tropomyosin, and F-actin ⁴⁶⁻⁴⁷. The consequences of their interactions are not known, especially *in vivo*, but their prominent roles in both filopodia formation and FA maturation ⁴⁸⁻⁵⁰, may yet prove to be influential in delivering the enhance migratory activities, as well as filopodial organisation induced by S100A4.

Acknowledgments

The authors would like to thank Kevin Küpper for great technical support and helpful discussions, along with Ms. Charlotte Bland and ARCHA at Aston University for support related to the work using confocal microscopy. Special thanks are also due to Georg Dreissen for help with the gray average analysis of the different actin staining.

References

1. Kirfel G, Rigort A, Borm B, Herzog V. Cell migration: mechanisms of rear detachment and the formation of migration tracks. *Eur J Cell Biol* 2004; 83:717-24.
2. Pollard TD, Borisy GG. Cellular motility driven by assembly and disassembly of actin filaments. *Cell* 2003; 112:453-65.
3. Mallavarapu A, Mitchison T. Regulated actin cytoskeleton assembly at filopodium tips controls their extension and retraction. *J Cell Biol* 1999; 146:1097-106.
4. Vignjevic D, Kojima S, Aratyn Y, Danciu O, Svitkina T, Borisy GG. Role of fascin in filopodial protrusion. *J Cell Biol* 2006; 174:863-75.
5. Partridge MA, Marcantonio EE. Initiation of attachment and generation of mature focal adhesions by integrin-containing filopodia in cell spreading. *Mol Biol Cell* 2006; 17:4237-48.
6. Schafer C, Borm B, Born S, Mohl C, Eibl EM, Hoffmann B. One step ahead: role of filopodia in adhesion formation during cell migration of keratinocytes. *Exp Cell Res* 2009; 315:1212-24.
7. Schafer C, Born S, Mohl C, Houben S, Kirchgessner N, Merkel R, et al. The key feature for early migratory processes: Dependence of adhesion, actin bundles, force generation and transmission on filopodia. *Cell Adh Migr* 2010; 4:215-25.
8. Nemethova M, Auinger S, Small JV. Building the actin cytoskeleton: filopodia contribute to the construction of contractile bundles in the lamella. *J Cell Biol* 2008; 180:1233-44.
9. Zaidel-Bar R, Itzkovitz S, Ma'ayan A, Iyengar R, Geiger B. Functional atlas of the integrin adhesome. *Nat Cell Biol* 2007; 9:858-67.
10. Wolfenson H, Bershadsky A, Henis YI, Geiger B. Actomyosin-generated tension controls the molecular kinetics of focal adhesions. *J Cell Sci* 2011; 124:1425-32.
11. Parsons JT, Horwitz AR, Schwartz MA. Cell adhesion: integrating cytoskeletal dynamics and cellular tension. *Nat Rev Mol Cell Biol* 2010; 11:633-43.
12. Cohen DM, Kutscher B, Chen H, Murphy DB, Craig SW. A conformational switch in vinculin drives formation and dynamics of a talin-vinculin complex at focal adhesions. *J Biol Chem* 2006; 281:16006-15.
13. Vicente-Manzanares M, Koach MA, Whitmore L, Lamers ML, Horwitz AF. Segregation and activation of myosin IIB creates a rear in migrating cells. *J Cell Biol* 2008; 183:543-54.
14. Totsukawa G, Yamakita Y, Yamashiro S, Hartshorne DJ, Sasaki Y, Matsumura F. Distinct roles of ROCK (Rho-kinase) and MLCK in spatial regulation of MLC phosphorylation for assembly of stress fibers and focal adhesions in 3T3 fibroblasts. *J Cell Biol* 2000; 150:797-806.
15. Totsukawa G, Wu Y, Sasaki Y, Hartshorne DJ, Yamakita Y, Yamashiro S, et al. Distinct roles of MLCK and ROCK in the regulation of membrane protrusions and focal adhesion dynamics during cell migration of fibroblasts. *J Cell Biol* 2004; 164:427-39.
16. Ford HL, Salim MM, Chakravarty R, Aluiddin V, Zain SB. Expression of Mts1, a metastasis-associated gene, increases motility but not invasion of a nonmetastatic mouse mammary adenocarcinoma cell line. *Oncogene* 1995; 11:2067-75.
17. Ford HL, Silver DL, Kachar B, Sellers JR, Zain SB. Effect of Mts1 on the structure and activity of nonmuscle myosin II. *Biochemistry* 1997; 36:16321-7.
18. Kriajevska MV, Cardenas MN, Grigorian MS, Ambartsumian NS, Georgiev GP, Lukanidin EM. Non-muscle myosin heavy chain as a possible target for protein encoded by metastasis-related mts-1 gene. *J Biol Chem* 1994; 269:19679-82.

19. Zhang S, Wang G, Fernig DG, Rudland PS, Webb SE, Barraclough R, et al. Interaction of metastasis-inducing S100A4 protein in vivo by fluorescence lifetime imaging microscopy. *Eur Biophys J* 2005; 34:19-27.
20. Li ZH, Spektor A, Varlamova O, Bresnick AR. Mts1 regulates the assembly of nonmuscle myosin-IIA. *Biochemistry* 2003; 42:14258-66.
21. Dulyaninova NG, Malashkevich VN, Almo SC, Bresnick AR. Regulation of myosin-IIA assembly and Mts1 binding by heavy chain phosphorylation. *Biochemistry* 2005; 44:6867-76.
22. Jenkinson SR, Barraclough R, West CR, Rudland PS. S100A4 regulates cell motility and invasion in an in vitro model for breast cancer metastasis. *Br J Cancer* 2004; 90:253-62.
23. Li ZH, Bresnick AR. The S100A4 metastasis factor regulates cellular motility via a direct interaction with myosin-IIA. *Cancer Res* 2006; 66:5173-80.
24. Ismail T, Fernig DG, Rudland PS, Terry CJ, Wang G, Barraclough R. The basic C-terminal amino acids of calcium-binding protein S100A4 promote metastasis. *Carcinogenesis* 2008.
25. Ismail TM, Zhang S, Fernig DG, Gross S, Martin-Fernandez ML, See V, et al. Self-association of calcium-binding protein S100A4 and metastasis. *J Biol Chem* 2010; 285:914-22.
26. Helfman DM, Kim EJ, Lukanidin E, Grigorian M. The metastasis associated protein S100A4: role in tumour progression and metastasis. *Br J Cancer* 2005; 92:1955-8.
27. Rudland PS, Platt-Higgins A, El-Tanani M, De Silva Rudland S, Barraclough R, Winstanley JH, et al. Prognostic significance of the metastasis-associated protein osteopontin in human breast cancer. *Cancer Res* 2002; 62:3417-27.
28. Davies BR, Davies MP, Gibbs FE, Barraclough R, Rudland PS. Induction of the metastatic phenotype by transfection of a benign rat mammary epithelial cell line with the gene for p9Ka, a rat calcium-binding protein, but not with the oncogene EJ-ras-1. *Oncogene* 1993; 8:999-1008.
29. Lloyd BH, Platt-Higgins A, Rudland PS, Barraclough R. Human S100A4 (p9Ka) induces the metastatic phenotype upon benign tumour cells. *Oncogene* 1998; 17:465-73.
30. Zhang S, Wang G, Liu D, Bao Z, Fernig DG, Rudland PS, et al. The C-terminal region of S100A4 is important for its metastasis-inducing properties. *Oncogene* 2005; 24:4401-11.
31. Dunnington DJ, Hughes CM, Monaghan P, Rudland PS. Phenotypic instability of rat mammary tumor epithelial cells. *J Natl Cancer Inst* 1983; 71:1227-40.
32. Andersen K, Nesland JM, Holm R, Florenes VA, Fodstad O, Maelandsmo GM. Expression of S100A4 combined with reduced E-cadherin expression predicts patient outcome in malignant melanoma. *Mod Pathol* 2004; 17:990-7.
33. Kimura K, Endo Y, Yonemura Y, Heizmann CW, Schafer BW, Watanabe Y, et al. Clinical significance of S100A4 and E-cadherin-related adhesion molecules in non-small cell lung cancer. *Int J Oncol* 2000; 16:1125-31.
34. Rudland PS, Platt-Higgins A, Renshaw C, West CR, Winstanley JH, Robertson L, et al. Prognostic significance of the metastasis-inducing protein S100A4 (p9Ka) in human breast cancer. *Cancer Res* 2000; 60:1595-603.
35. Yonemura Y, Endou Y, Kimura K, Fushida S, Bandou E, Taniguchi K, et al. Inverse expression of S100A4 and E-cadherin is associated with metastatic potential in gastric cancer. *Clin Cancer Res* 2000; 6:4234-42.
36. Ambartsumian NS, Grigorian MS, Larsen IF, Karlstrom O, Sidenius N, Rygaard J, et al. Metastasis of mammary carcinomas in GRS/A hybrid mice transgenic for the mts1 gene. *Oncogene* 1996; 13:1621-30.

37. Takenaga K, Nakamura Y, Endo H, Sakiyama S. Involvement of S100-related calcium-binding protein pEL98 (or mts1) in cell motility and tumor cell invasion. *Jpn J Cancer Res* 1994; 85:831-9.
38. Takenaga K, Nakamura Y, Sakiyama S. Expression of antisense RNA to S100A4 gene encoding an S100-related calcium-binding protein suppresses metastatic potential of high-metastatic Lewis lung carcinoma cells. *Oncogene* 1997; 14:331-7.
39. Bjornland K, Winberg JO, Odegaard OT, Hovig E, Loennechen T, Aasen AO, et al. S100A4 involvement in metastasis: deregulation of matrix metalloproteinases and tissue inhibitors of matrix metalloproteinases in osteosarcoma cells transfected with an anti-S100A4 ribozyme. *Cancer Res* 1999; 59:4702-8.
40. Kim EJ, Helfman DM. Characterization of the metastasis-associated protein, S100A4. Roles of calcium binding and dimerization in cellular localization and interaction with myosin. *J Biol Chem* 2003; 278:30063-73.
41. Hotulainen P, Lappalainen P. Stress fibers are generated by two distinct actin assembly mechanisms in motile cells. *J Cell Biol* 2006; 173:383-94.
42. Medeiros NA, Burnette DT, Forscher P. Myosin II functions in actin-bundle turnover in neuronal growth cones. *Nat Cell Biol* 2006; 8:215-26.
43. Betapudi V. Myosin II motor proteins with different functions determine the fate of lamellipodia extension during cell spreading. *PLoS ONE* 2010; 5:e8560.
44. Tokuo H, Mabuchi K, Ikebe M. The motor activity of myosin-X promotes actin fiber convergence at the cell periphery to initiate filopodia formation. *J Cell Biol* 2007; 179:229-38.
45. Schafer C, Born S, Mohl C, Houben S, Kirchgessner N, Merkel R, et al. The key feature for early migratory processes: Dependence of adhesion, actin bundles, force generation and transmission on filopodia. *Cell Adh Migr* 2010; 4.
46. Takenaga K, Nakamura Y, Sakiyama S, Hasegawa Y, Sato K, Endo H. Binding of pEL98 protein, an S100-related calcium-binding protein, to nonmuscle tropomyosin. *J Cell Biol* 1994; 124:757-68.
47. Watanabe Y, Usada N, Minami H, Morita T, Tsugane S, Ishikawa R, et al. Calvasculin, as a factor affecting the microfilament assemblies in rat fibroblasts transfected by src gene. *FEBS Lett* 1993; 324:51-5.
48. Creed SJ, Desouza M, Bamburg JR, Gunning P, Stehn J. Tropomyosin isoform 3 promotes the formation of filopodia by regulating the recruitment of actin-binding proteins to actin filaments. *Exp Cell Res* 2011; 317:249-61.
49. Gupton SL, Anderson KL, Kole TP, Fischer RS, Ponti A, Hitchcock-DeGregori SE, et al. Cell migration without a lamellipodium: translation of actin dynamics into cell movement mediated by tropomyosin. *J Cell Biol* 2005; 168:619-31.
50. Bach CT, Schevzov G, Bryce NS, Gunning PW, O'Neill GM. Tropomyosin isoform modulation of focal adhesion structure and cell migration. *Cell Adh Migr* 2010; 4:226-34.

Legend

Figure 1: Full length S100A4 overexpression enhances the rate of wound closure.

Rama 37 control cells, cells expressing wild type S100A4, S100A4 Δ 2, and S100A4 Δ 6 were grown for 24 hrs in 24 well plates prior to a wound healing assay. A) Representative time-lapse images of Rama 37 cells scratch assays immediately after the scratches had been made and then after 8 hrs. Scale bar = 200 μ m. B) Quantification of wound closure. A similar experiment was carried out using the CellIQ system and rates of wound healing were determined. Data shown are means \pm s.e., * p < 0.05 or ** p < 0.001.

Figure 2: Overexpression of wild type S100A4 but not the C-terminal truncated forms Δ 2 or Δ 6 prevents formation of mature focal adhesions.

Rama 37 Control cells (A-A'), or cells expressing wild type S100A4 cells (B-B'), S100A4- Δ 2 (C-C'), and S100A4- Δ 6 (D-D') were grown for 48 hrs on glass coverslips coated with fibronectin prior to fixing and staining by immunofluorescence for paxillin and actin. Cells were mounted and viewed using confocal microscopy. Panels A', B', C' and D' correspond to focused regions of the cell. Scale bar = 50 μ m.

Figure 3: High levels of full length S100A4 reduce the number of adhered filopodia.

Rama 37 control cells (A-A'), or cells expressing wild type S100A4 (B-B'), S100A4 Δ 2 (C-C'), and S100A4 Δ 6 (D-D') were grown for 48 hrs on glass coverslips coated with fibronectin prior to fixing and staining by immunofluorescence for fascin or actin. Cells were mounted and viewed using confocal microscopy. Panels A', B', C' and D' correspond to focused regions of the cell. Scale bar = 50 μ m.

Figure 4: Differentiating matured and nascent focal adhesion in Rama 37 cells

Control Rama 37 cells transfected with pGZ21 GFP-vinculin expressing plasmid were seeded on fibronectin coated coverslips for 24 hrs before analysis. Cells were analyzed over a time

period of 20 minutes in phase contrast (A) and fluorescence (B). Red box in the overview indicates the zoomed area shown in the time series. Time points are recorded in seconds. The black arrow highlights the same filopodial position over time. For better visualisation, phase contrast images were sharpened and GFP-images were background-subtracted and the contrast was adjusted before overlaying the images. Scale bar = 20 μ m.

Figure 5. Establishment of stably adhered filopodia, retraction fibres and unstable filopodia in Rama 37 cells

Rama 37 S100A4- Δ 6 cells transfected with pGZ21 GFP-vinculin expressing plasmid were seeded on fibronectin coated coverslips for 24 hrs before analysis. Cells were analysed over a 20 minutes time period in phase contrast and fluorescence to quantify stably adhered filopodia (white arrow, **A**), retraction fibres (**B**) and unstable filopodia (yellow arrow, **C**). Area **A** was enlarged to show the formation of stable filopodia (top panel), the subsequent maturation of FA (middle panel) and the overlay of both time lapse images (bottom panel) over time (**A**). Area **B** was enlarged with a white line drawn above to show the retracting FA right behind the retraction fibres over time (**B**). Area **C** was enlarged to show the unstable formation of filopodia over time (**C**). For **A**, **B** and **C**, the top panel is shown in phase contrast, the middle panel in fluorescence and the bottom panel as overlays of both images. Time points are given in seconds. Note that the time lapse has shorter intervals for **C** whereas **A** and **B** have a similar time lapse. First image of all analysis corresponds to the main figure (time zero) and then subsequent time lapse images are shown. For better visualisation, phase contrast images were sharpened and GFP-images were background-subtracted and enhanced in contrast before overlaying the images. Scale bar = 20 μ m.

Supplementary Video 1. Images of Control Rama 37 cells transfected with pGZ21 GFP-vinculin expressing plasmid were captured with confocal microscopy (LSM710, Zeiss) over duration of 20 min with 10s intervals. For better visualisation, images were optimised with ImageJ (background-subtraction, contrast enhancement and sharpened).

Supplementary Video 2. Images of Rama 37 S100A4WT cells transfected with pGZ21 GFP-vinculin expressing plasmid were captured with confocal microscopy (LSM710, Zeiss)

over duration of 20 min with 10s intervals. For better visualisation, images were optimised with ImageJ (background-subtraction, contrast enhancement and sharpened).

Supplementary Video 3. Images of Rama 37 S100A4 Δ 2 cells transfected with pGZ21 GFP-vinculin expressing plasmid were captured with confocal microscopy (LSM710, Zeiss) over duration of 20 min with 10s intervals. For better visualisation, images were optimised with ImageJ (background-subtraction, contrast enhancement and sharpened).

Supplementary Video 4. Images of Rama 37 S100A4 Δ 6 cells transfected with pGZ21 GFP-vinculin expressing plasmid were captured with confocal microscopy (LSM710, Zeiss) over duration of 20 min with 10s intervals. For better visualisation, images were optimised with ImageJ (background-subtraction, contrast enhancement and sharpened).

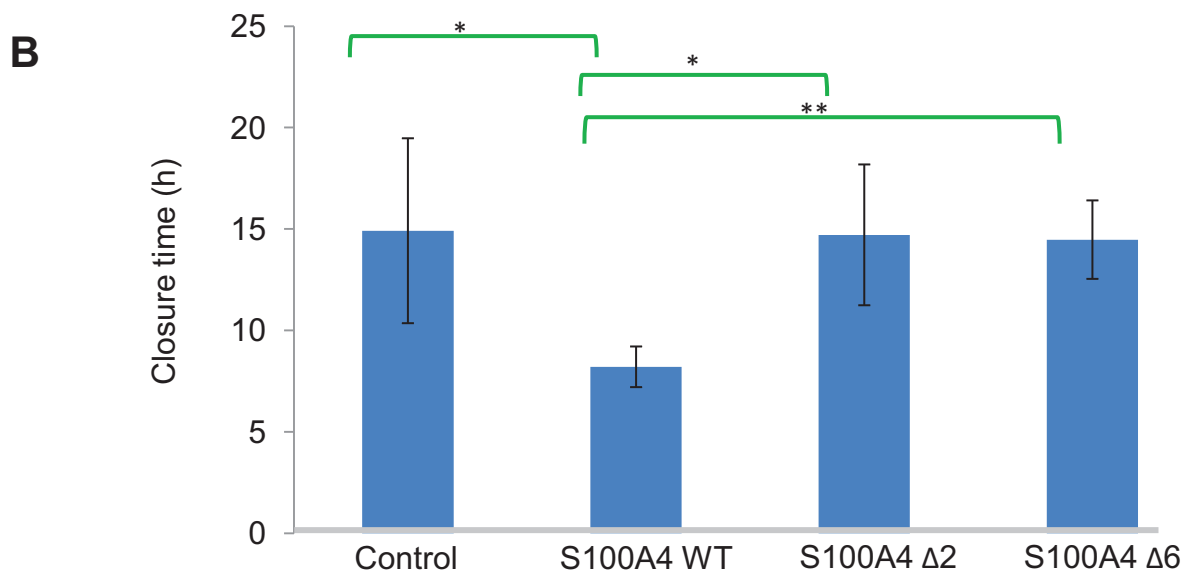
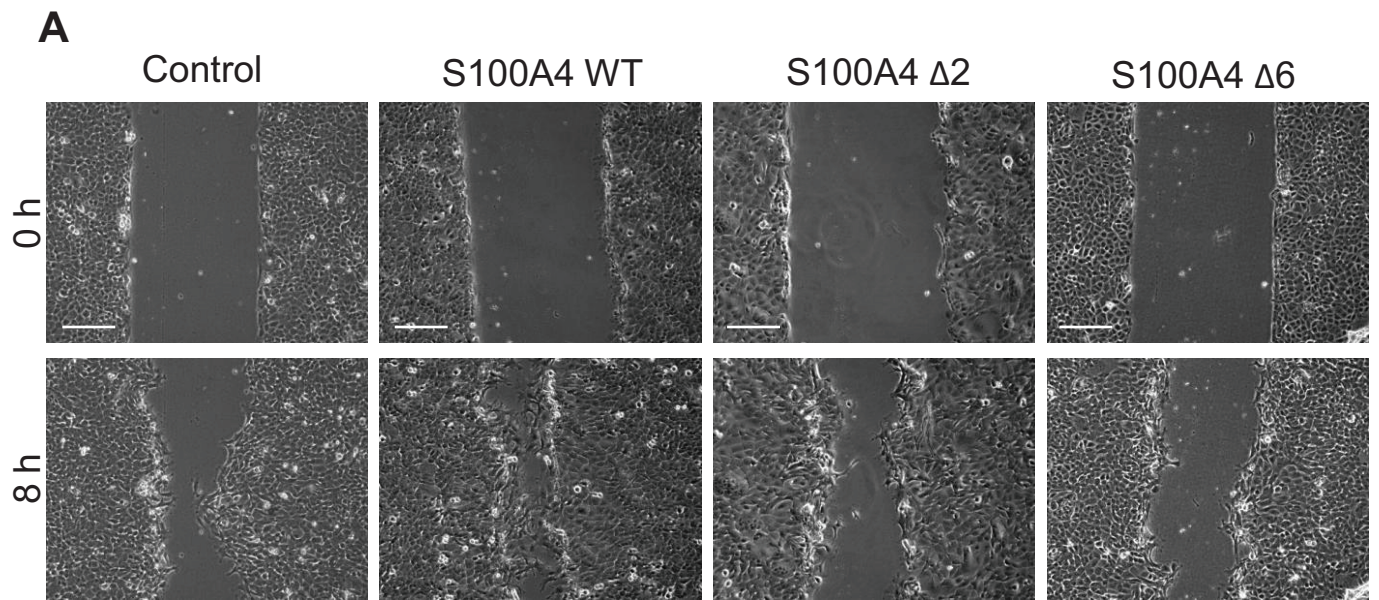


Figure 1

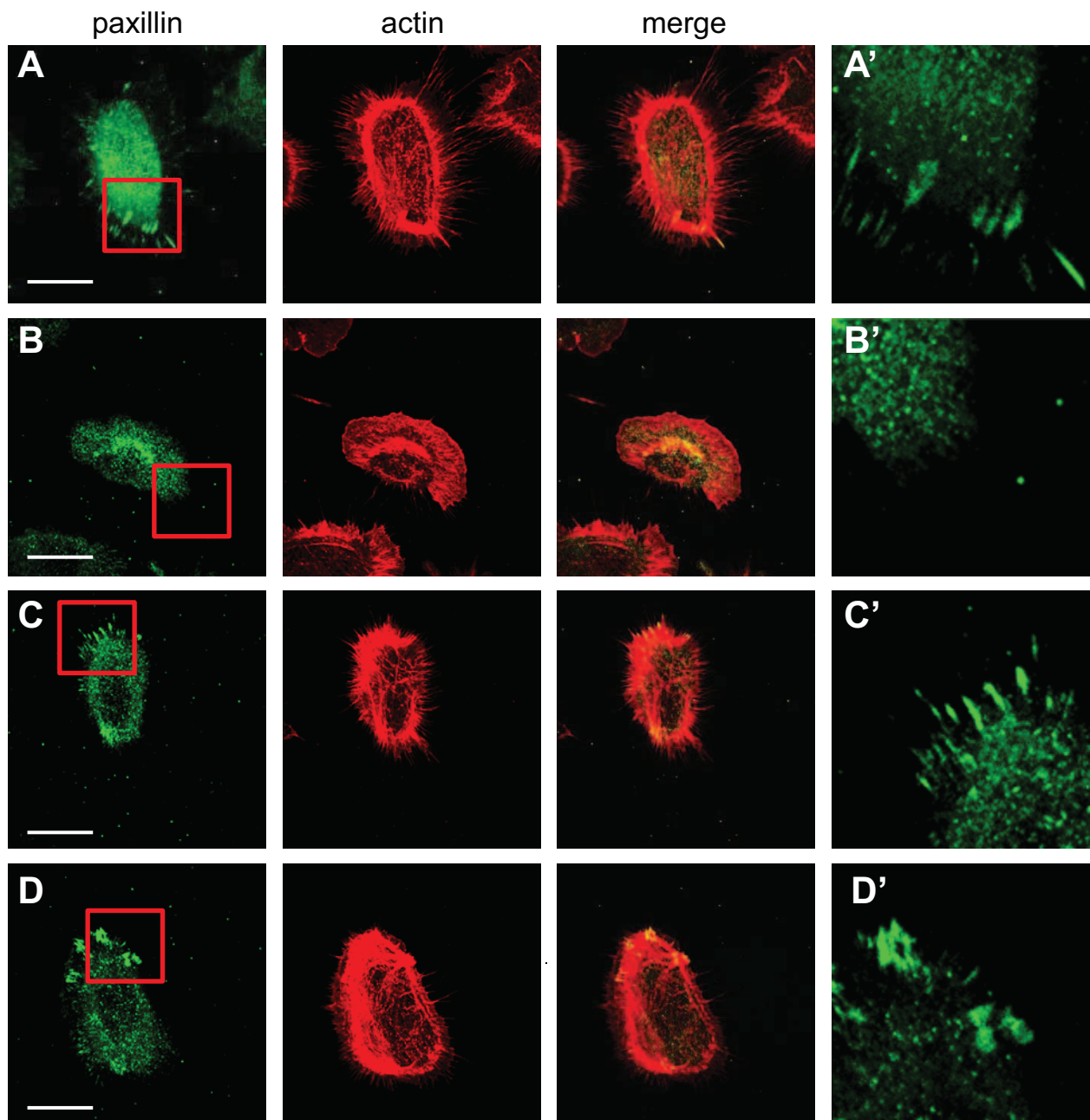


Figure 2

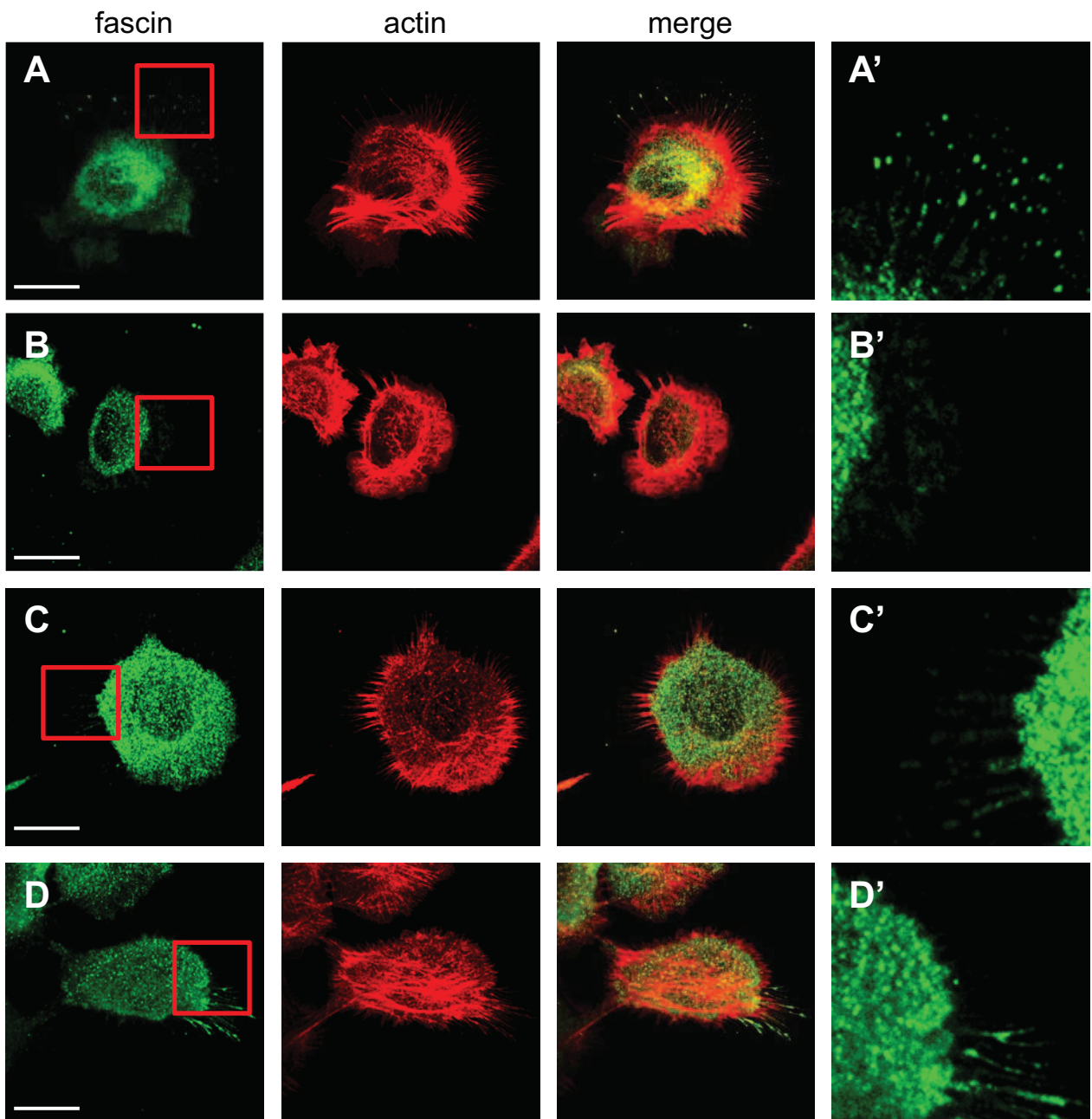


Figure 3

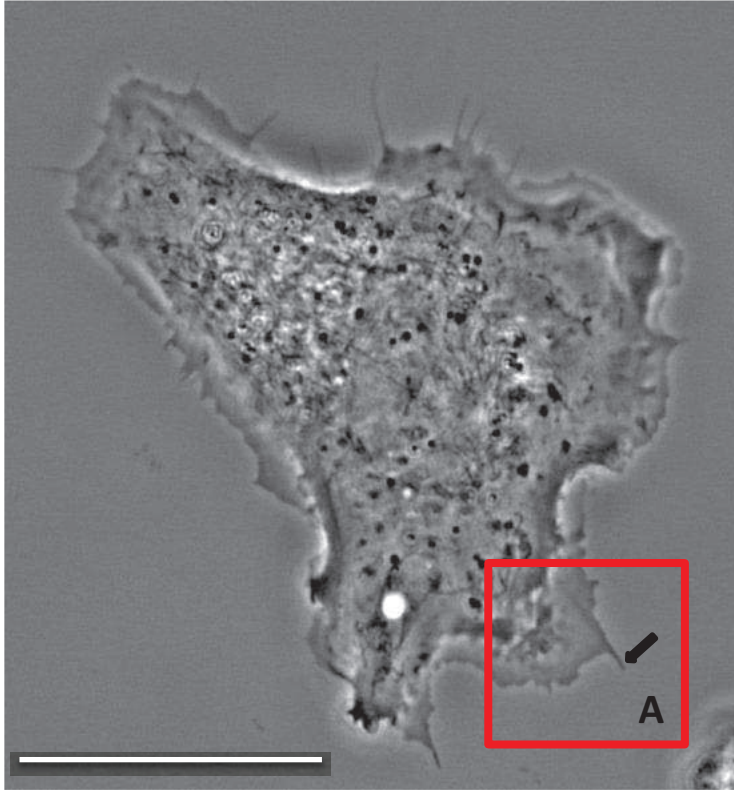
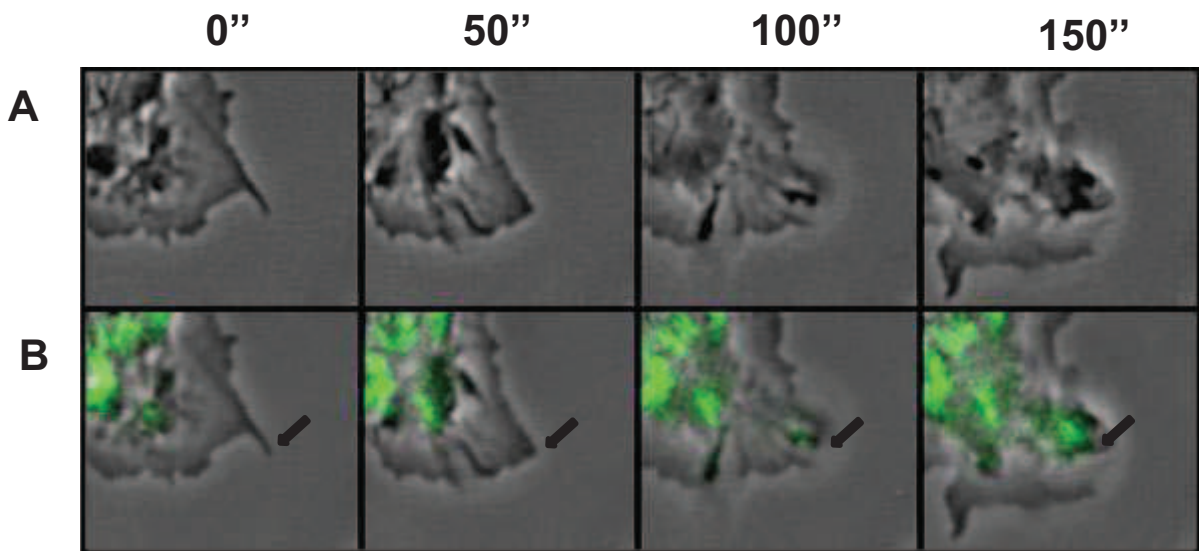


Figure 4



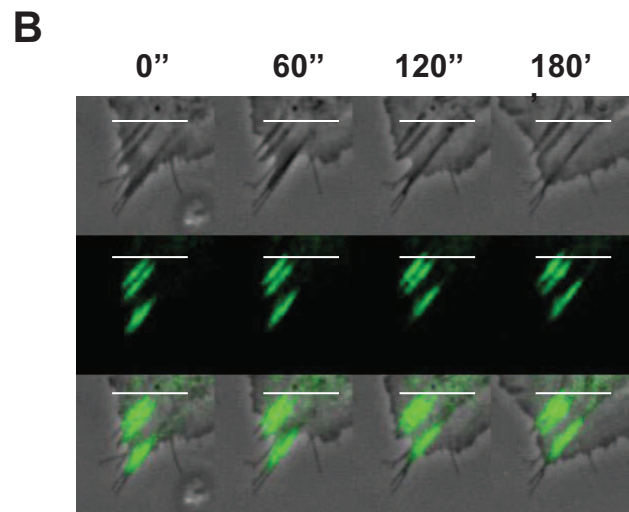
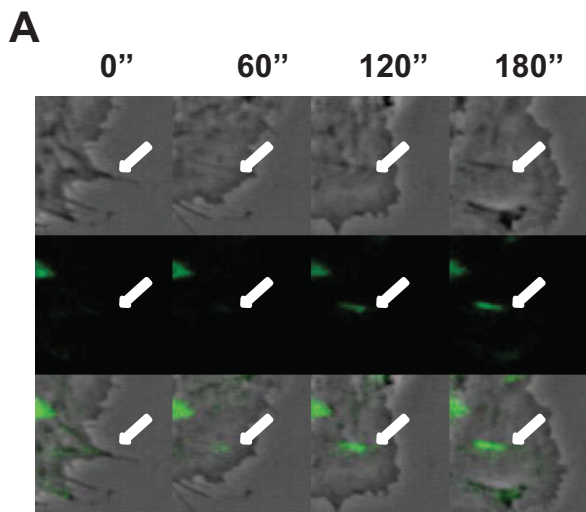
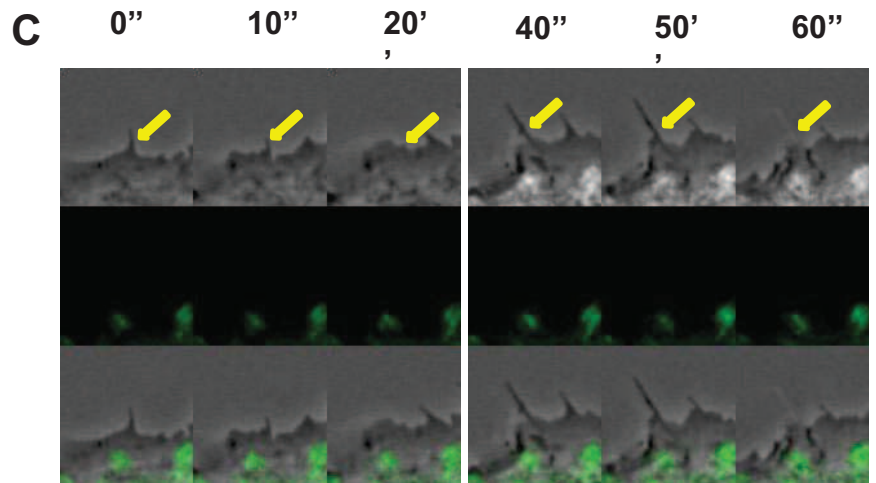
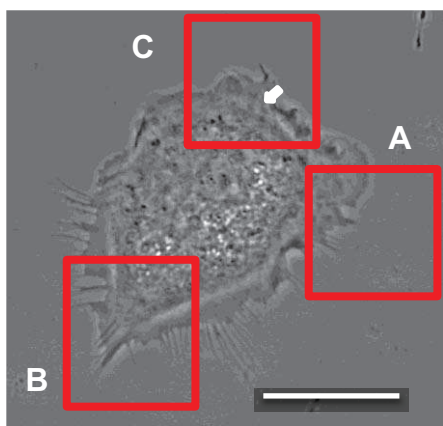


Figure 5

Table 1: Expression of wild type S100A4 reduces the number of projections per cell

Cell lines	Number of projections per cell \pm s.e. (n=5)	<i>P</i> -value ^a	<i>P</i> -value ^b	<i>P</i> -value ^c
Rama 37 Control	41.20 \pm 8.58			
Rama 37 S100A4 WT	3.50 \pm 1.52	0.0001		
Rama 37 S100A4 Δ 2	31.57 \pm 11.31	0.0708	0.00004	
Rama 37 S100A4 Δ 6	19.71 \pm 8.69	0.0008	0.0004	0.0062

Rama 37 control cells, cells expressing wild type S100A4, S100A4 Δ 2, and S100A4 Δ 6 were fixed and stained for fascin and actin after seeding on fibronectin coated coverslips and growth for 48 hours. Data shown are means \pm s.e. corresponds to the average number of projection containing fascin observed per cells.

^a *P*-value obtain from Student t-Test where total number of projections present in Rama 37 Control were compared to Rama 37 S100A4WT, Rama 37 S100A4 Δ 2 and Rama 37 S100A4 Δ 6

^b *P*-value obtain from Student t-Test where total number of projections present in Rama 37 S100A4WT were compared to Rama 37 S100A4 Δ 2 and Rama 37 S100A4 Δ 6

^c *P*-value obtain from Student t-Test where total number of projections present in Rama 37 S100A4 Δ 2 were compared to Rama 37 S100A4 Δ 6

Table 2. Expression of wild type S100A4 protein causes overall reduction in focal adhesion

Cell lines (protein encoded in expression vector)	Number of focal adhesion present (over 20 minutes) \pm s.e. (n=5)	P- value ^a	Number of focal adhesion formed (within 20 minutes) \pm s.e. (n=5)	P- value ^b	Number of filopodia present \pm s.e. (n=9)	P- value ^c
Rama 37 Control	89.4 \pm 13.4	0.0028	14.4 \pm 2.1	0.0705	10.9 \pm 2.71	0.0271
Rama 37 S100A4 WT	50.2 \pm 11.5		11.4 \pm 3.5		17.3 \pm 7.2	
Rama 37 S100A4 Δ2	93.6 \pm 6.3	0.0019	28.2 \pm 6.9	0.0110	14.6 \pm 6.9	0.5460
Rama 37 S100A4 Δ6	83.6 \pm 12.1	0.0326	23.6 \pm 6.6	0.0041	10.9 \pm 4.5	0.0307

Rama 37 control cells, cells expressing wild type S100A4, S100A4 Δ 2, and S100A4 Δ 6 were transfected with pGZ21 GFP-vinculin expressing plasmid and then seeded on fibronectin coated coverslips for 24 hrs before analysis. Cells were analysed over a 20 minutes time period in phase contrast and fluorescence. Quantification of the total numbers of FA present, newly formed FA within the 20 minute time frame, as well as the number of forming filopodia was carried out using the image J software.

^a P value obtain from Student t-Test where total number of focal adhesions present during 20 minutes live cell imaging of Rama 37 Control, Rama 37 S100A4 Δ 2 and Rama 37 S100A4 Δ 6 were compared to those of Rama 37 S100A4 WT.

^b P value obtain from Student t-Test where total number of focal adhesions formed during 20 minutes live cell imaging of Rama 37 Control, Rama 37 S100A4 Δ 2 and Rama 37 S100A4 Δ 6 were compared to those formed during imaging of Rama 37 S100A4 WT.

^c P value obtain from Student t-Test where total number of filopodia present on Rama 37 Control, Rama 37 S100A4 Δ 2 and Rama 37 S100A4 Δ 6 were compared to those on Rama 37 S100A4 WT.